S. Cerri, M.A. Bohn, K. Menke, L. Galfetti
*Aging of ADN Rocket Propellant Formulations with Desmophen-Based Elastomer Binder*
Propellants, Explosives, Pyrotechnics, Vol. 39, N. 4, 2014, p. 526-537
doi:10.1002/prep.201300124

# Aging of ADN Rocket Propellant Formulations with Desmophen®-Based Elastomer Binder

Sara Cerri[1], Manfred A. Bohn[2], Klaus Menke[2], Luciano Galfetti[3]

1 Independent Consultant, 28060, Cureggio, Italy
2 Fraunhofer Institut fuer Chemische Technologie (ICT), 76318, Pfinztal-Berghausen, Germany
3 Dipartimento di Scienze e Tecnologie Aerospaziali, Politecnico di Milano, 20156, Milano, Italy

## Abstract

Desmophen® binder-based rocket propellant formulations containing ammonium dinitramide (ADN) and different fuel filler types (Al, HMX) were manufactured and investigated. Desmophen® D2220 is a polyesterpolyol. Polyesters are seen as a binder possibility, because of the relatively low temperature of the glass transition region compared to polyether-based prepolymers such as GAP. The analogous formulations with AP instead of ADN were also included for comparison. The aging was followed by SEM, DSC, and DMA measurements. The accelerated aging program was developed on the principle of thermal equivalent load and the generalized van't Hoff rule with a scaling factor equal to F=2.9. The aging was performed in air (RH<10 %) at temperature values between 65 and 85 °C and aging times adjusted to a thermal equivalent load of 15 years at 25 °C. DMA measurements of the aged ADN/Desmophen®-based propellants identified changes in the loss factor curve. In contrast to HTPB-Al-AP rocket propellant formulations, the loss factor curve of the ADN formulations with Desmophen®-based elastomer binder shows only one main apparent peak. The loss factor curves were modeled with exponentially modified Gaussian functions, which have revealed the presence of a second hidden peak. It was found that the aging could be characterized by the time-temperature dependence of the areas of the hidden peak. The area increased with aging, which is explained by scissioning of the polymer in the shell around the ADN particles. By this process the strength is reduced, which was recognized by the decrease in storage shear modulus.

# 1 Introduction

In recent years, smokeless, low-signature, environmentally friendly, or reduced polluting solid rocket propellant formulations have gained more and more attention for defense and space applications [1-9]. The reasons are: (i) to have low signature propellants in tactical rockets to reduce their identification by plume diagnostics [3–5, 7, 9]; (ii) environmental issues due to perchlorate contamination 1, 2 and hydrochloric acid produced by the firing of ammonium perchlorate (AP)-based propellants currently used in the majority of the rocket motors for tactical and ballistic-strategic systems and space launch applications 2–4; (iii) additional concerns about the safe and pollution-free disposal of energetic materials are rising.

The research community has started with more intensity to consider ammonium dinitramide (ADN) as a potential AP substitute for smokeless and higher performance rocket propellants as well as to consider the "green" aspect of ADN. In 2011, a consortium of several European partners awarded a

FP7 grant from the European Union with a project called HISP (High Performance Solid Propellants for In-Space Propulsion) [2]. The FP7 project focuses on the development of high performance solid rocket propellants using ADN, energetic binders and additives. In the literature most of the efforts have been focused on the thermal decomposition, ballistic performance evaluation and combustion characterization of ADN-based propellant formulations [3–6]. Relatively few works discussed the mechanical characterization [7–9].
In this study, the aging of Desmophen®-based propellant formulations containing ADN and different filler types (aluminum powder, HMX particles) was investigated with differential scanning calorimetry (DSC) measurements, dynamic mechanical analysis (DMA), and scanning electron microscopy (SEM). The choice of polyester-based polyurethanes as binders considers the fact that they have, in general, a better rubber-to-glass transition behavior than polyether-based polyurethanes. HTPB-based binders are considered to have insufficient compatibility with ADN. One of the main aspect of this work was to look on such a polyester based binder and its behavior together with ADN. Glycidylazide polymer (GAP) as binder cured with bispropargylsuccinate (BPS) and Desmodur® N100 was investigated in a previous study [7] but those GAP-based propellant formulations showed not satisfactory mechanical properties and strong dewetting phenomena. Moreover, their mass loss measurements revealed an acceleratory behavior higher than the Desmophen®-based propellant formulations. GAP is formally a polypropylene oxide based energetic polyurethane prepolymer. Because of its mainly linear chain and the relatively strong energetic interactions between the chains such polyethers have generally a glass-to-rubber transition temperature higher than polyesters, because polyesters can create more free volume with the ester groups by causing the kinking of the main chain and additional rotational freedom is introduced at the ester group. Aging of composite propellants is generally governed by the degradation of the binder, e.g. for HTPB/IPDI-based binders the decomposition by oxygen attack and by mechanical overload are the essential degradation mechanisms. In principle, ADN-based composite propellants show the same aging effects as the AP-based ones, but a severe additional aging can be caused by the aggressive oxidizing ability of ADN. In order to study this influence, comparisons with AP analogues have been made. A further main aspect of the work was to investigate how ADN influences the aging of the propellant formulations. For this the evaluation of the loss factor determined with DMA is an important method, because with HTPB-AP-Al composite rocket propellant (CRP) formulations parts of their loss factor have proven to be a valuable aging indicator. The temperature range of the accelerated aging was between 65 °C and 85 °C with aging times adjusted to a thermal equivalent load of 15 years at 25 °C.

# 2 Experimental Section

## 2.1 Formulations

Several Desmophen® -D2200-based propellant formulations, manufactured at Fraunhofer ICT, were investigated. Details of the formulations are shown in Table 1. For convenience and in congruence with the preceding paper [7], they are named *y*-D2200xx and depending on the considered oxidizer, the prefix ADN or AP substitutes the letter *y*. But because in this paper only the D2200 binder is used its indication in the naming is further on omitted. The formulation numbers can be added by replacing the xx. The first two formulations of Table 1 contain ADN as oxidizer and the same total solid load (66 m.-%) and the same additional filler content (10 m.-%) but different filler type: ADN-V142 contains HMX, whereas ADN-V144 contains aluminum. Therefore the effect of the filler type with aging can be investigated. The two AP-based formulations have the same solid load but with bimodal AP particles: AP-11 contains Al, while AP-12 contains HMX. AP-11 corresponds to ADN-V144 and AP-12 to ADN-V142.

Table 1. Composition in mass-% (m.-%) of the *y*-xx formulations. AP-11 corresponds to ADN-V144, whereas AP-12 corresponds to ADN-V142.

| Components | Unit | ADN-V142 | ADN-V144 | AP-11 | AP-12 |
|---|---|---|---|---|---|
| ADN prills 106 µm | Mass-% | 56.00 | 56.00 | – | – |
| AP 45 µm | Mass-% | – | – | 18.66 | 18.66 |
| AP 200 µm | Mass-% | – | – | 37.34 | 37.34 |
| HMX 5 µm | Mass-% | 10.00 | – | – | 10.00 |
| Al 8 µm | Mass-% | – | 10.00 | 10.00 | – |
| Desmophen® D2200 | Mass-% | 17.42 | 17.42 | 17.42 | 17.42 |
| TMETN+0.5 % 2-NDPA | Mass-% | 10.80 | 10.80 | 10.80 | 10.80 |
| HX-880 | Mass-% | 0.14 | 0.14 | 0.14 | 0.14 |
| Stabilizers | Mass-% | 1.60 | 1.60 | 1.60 | 1.60 |
| Desmodur® N3400 | Mass-% | 4.04 | 4.04 | 4.04 | 4.04 |
| Solid load | Mass-% | 66.00 | 66.00 | 66.00 | 66.00 |
| Plasticizer of binder | Mass-% | 33.33 | 33.33 | 33.33 | 33.33 |
| $R_{eq}$ (NCO/OH) | – | 1.00 | 1.00 | 0.99 | 0.99 |
| $\rho_{th}$ | g cm$^{-3}$ | 1.589 | 1.628 | 1.689 | 1.646 |
| O.B. | % | −30.89 | −37.63 | −26.27 | −32.97 |

Formulations were prepared in a vertical kneader (Drais T FHG, Germany) with 5 L volume and cured in an electrical oven cabinet (company Memmert, Germany).
The ADN-xx formulations were processed at 50 °C and cured 2 d at 60 °C. The AP-xx formulations were processed at 50 °C and cured 2 d at 60 °C. All formulations contain 0.14 m.-% of bonding agent of type HX-880 (company Mach I, Inc., King of Prussia, PA, USA). The ADN prills were manufactured at Fraunhofer ICT with a mean particle size of 106 µm (particle size ranges from 60–120 µm). Uncoated and unstabilized prills were used.

## 2.2 Sample Preparation and Aging Conditions

Samples were aged isothermally at temperatures in the range of 65–85 °C in air (RH<10 %) and in load-free conditions (no effect of stress and/or strain caused by the motor case are occurring) to simulate 15 years of aging at 25 °C (Table 2). The thermal accelerated aging program was carried out in PID temperature controlled (±0.3 °C) aging oven; their design is based on former company Julius Peters KG, Berlin, Germany. To establish the aging plan the principle of Thermal Equivalent Load (TEL) was used together with the generalized van't Hoff rule (GvH) 10, using a scaling factor F=2.9 per 10 °C temperature change. The GvH formula can well reproduce a two-step decomposition mechanism often found with energetic materials (NC based propellants [11] and HTPB-based propellant formulations [12]). The value of the F factor depends on the activation energy range of the aging process, e.g. with activation energy values of about 80 to 120 kJ mol$^{-1}$ and a temperature range between 20 and 90 °C the scaling factor is about 3. The principles and handling of the extrapolation by the GvH and the choice of the appropriate F value are explained in [10]. The higher the activation energy, the higher is the F factor, the shorter are the aging times. Considering that the activation energies in ADN systems can be higher than with HTPB based formulations [12], a value of F moderately higher than the one used for the AP/HTPB-formulations investigated in a previous study with F=2.5 [13] was used, in order not to shorten too much the accelerated aging times.

Table 2. Applied accelerated aging conditions (time and temperature) simulating an in-service time period of up to 15 years at 25 °C.

| **Natural aging or in-service time periods** | | | |
|---|---|---|---|
| In-service temperature [°C] | In-service time period [years] | | |
| 25 | 5 | 10 | 15 |
| Accelerated aging conditions based on TEL with F=2.9 in GvH | | | |
| **Aging temperature [°C]** | **Aging time [a] [d]** | | |
| 85 | 4 | 8 | 12 |
| 80 | 6 | 12.5 | 20 |
| 70 | 15 | 30 | 45 |
| 65 | 23.5 | 47 | 70.5 |

a) The given aging times are rounded up.

The study focused on the accelerated aging of the surface-layer of solid rocket propellants, which means no "in core" analysis was intended. Therefore, the sampling did not follow the STANAG 4581 [14]. The specimen geometry was already the one suitable for the DMA measurements, which means small rectangular bars: 10 mm wide, 4 to 5 mm thick, 30 mm long. DMA samples were stored in glass tubes having ground glass stoppers. Stoppers were not fixed with a clamp and not sealed by grease. Twice a week, stoppers were removed to let fresh air flow inside. The relative humidity was below 10%.

## 2.3 Characterization Techniques

### 2.3.1 Dynamic Mechanical Analysis (DMA)

All DMA measurements were carried out in torsion mode using a DMA instrument of type ARES™ (Advanced Rheometric Expansion System) manufactured by former Rheometric Scientific Inc. (now belonging to Waters Inc., BU TA Instruments). A liquid nitrogen cooling accessory was used for the low and high temperature operations. The investigated temperature range was −80 to +80 °C, with heating up in steps of 1 °C $min^{-1}$ and a soak (equilibration) time of 28 s. Specimens were tested at four sinusoidally applied deformation frequencies: 0.1, 1, 10, 30 Hz. These propellants were softer than the HTPB/AP/Al-based ones investigated in a previous study [13] due to the used binder and the lower solid load. A strain control equal to 0.0012 was too low to obtain good results, especially at temperatures above room temperature. Therefore two strain controls were used: 0.00237 from −80 up to +15 °C, and 0.01 from +16 to +80 °C.
Measurement reproducibility of the ARES instrument is very high, so only one sample was used. In case of anomalous behavior a second measurement was performed. As a general rule, specimens were tested at least 1 h and 30 min after removal from the oven in order to reach room temperature and to avoid temperature inhomogeneities inside the sample.

### 2.3.2 DSC Measurements

DSC measurements were performed in nitrogen atmosphere using the DSC 2920 manufactured by TA Instruments (Newcastle, Delaware, USA). Small amounts of propellants (about 10 mg) were analyzed with heating rate of 10 °C $min^{-1}$. The purpose of these measurements was to investigate the glass transition temperature ($T_{g,DSC}$) of the materials and the presence or absence of secondary relaxation phenomena. The aging conditions of the samples were:

- (i) Unaged condition;
- (ii) 85 °C: 8, 12 days, in air;

- (iii) 80 °C: 12.5, 20 days, in air;
- (iv) 70 °C: 15, 30, 45 days, in air;
- (v) 65 °C: 23.5, 47 days, in air.

### 2.3.3 SEM Measurements

Scanning electron microscopy analyses were performed using the scanning electron microscope Supra 55 VP manufactured by company ZEISS, Germany. Some unstressed specimens of the ADN-V142 formulations were aged at 65 °C, 70 °C, 80 °C, in order to follow the surface modification due to the thermal load.

# 3 Results and Discussion

The investigated propellants have a lower solid load than the standard AP/HTPB-based formulations, whose typical values are between 75 and 85 m.-%. This was due to a technical limitation. ADN crystals are available in a needle shape, thus prilling techniques have been developed to convert the ADN crystals to spherical particles either in suspension in an inert fluid or in a gas stream. Because at the time of this study, multimodal ADN distributions were not available, the multipacking density approach could not be used and the only possibility to achieve higher solid load, density, and performance of the propellant formulations was to add a further fuel filler (HMX or Al). Recent results have shown that ADN particles with an adequate particle size can be produced by combining the micro reaction technique and the ADN emulsion crystallization [15].
ADN- and AP-based propellant formulations containing HMX or Al as filler type, different pre-polymers (GAP diol/triol, Desmophen®), plasticizers (BDNPA-F, TMETN), and curing agents (bispropargylsuccinate, Desmodur® N100, Desmodur® N3400), bonding agent such as HX-880 were investigated in a previous study [7, 16]. Formulations were characterized by tensile tests, SEM analysis, DMA measurements, and mass loss. In the following, a summary of the main conclusions is provided. The mechanical properties of the investigated GAP- and Desmophen®-based formulations were below the "state-of-the-art" formulations, represented by HTPB/AP/Al-based propellants ($\sigma_{corr}$>1 N mm$^{-2}$, $\varepsilon_{log}$≈0.25–0.30), but the Desmophen®-based ones showed higher maximum corrected stress values ($\sigma_{corr}$≈0.6 to 0.2–0.3 N mm$^{-2}$) and lower strain capability than the GAP-based formulations ($\varepsilon_{log}$≈0.05 to 0.13). The constitutive behavior of the ADN/GAP-based formulations was independent of the filler type, whereas the Desmophen®-based ones showed a strong dependence: the formulation containing HMX has a higher strain capability. DMA measurements revealed high glass transition temperature values for all the formulations. These values were 40 to 50 °C higher than the ones of the current HTPB/AP/Al-based formulations. But the ADN/polyesterurethane-based materials showed lower glass transition temperature values than the ADN/GAP-based formulations, approximately −33 °C vs. −28 to −25 °C, respectively. Finally, some information regarding the aging behavior was obtained with mass loss measurements. They revealed that the melting down of the GAP-based materials appears in half the time compared to the Desmophen®-based ones. Melting means the binder was decomposed. For these reasons, the aging investigation presented in this paper has only been focused on the Desmophen®-based propellant formulations.

## 3.1 DMA and DSC Investigations

The loss factor, tan(δ)=G″/G′ has been used to study the influence of the bonding agent on the transition regions [17], the influence of the plasticizer content [18], of post-curing [17] and of the aging of AP/HTPB-based formulations [13].

Figure 1 shows the baseline corrected loss factor curves of the unaged ADN-xx and AP-xx propellants tested at 0.1 Hz together with the binder with and without plasticizer (explanation of the baseline correction procedure will be provided later). Each formulation has only one apparent (deformation frequency dependent) peak, which has especially with the ADN-xx a type of tailing towards the high temperature side. This thermo-viscoelastic behavior differs from the one characterizing the AP/HTPB-based propellant formulations [13]. Values of tan(δ) of the y-xx formulations containing AP are higher than the ones containing ADN. Propellants containing HMX show higher loss factor values than the ones containing aluminum. The reduction of the maximum of tan(δ) with aluminum can be explained by the presence of more intense interactions between aluminum particles and binder, which causes a reduction in the polymer mobility. The surface of Al is polar by OH groups. This is not the case with HMX. These polar OH groups can form hydrogen bonds to the ester groups of the binder and moreover exert long-ranging electrostatic forces, which reduce the mobility already at somewhat higher temperature than HMX [7]. This explanation is in line with the $T_g$ values of the pure binder with and without plasticizer. The glass transition temperature $T_g$ derived from DMA measurements is taken as the temperature of the maximum of the loss factor peak. The binder with plasticizer is not disturbed by the electrostatic interactions with the fillers and has the lowest glass transition temperature and the highest intensity of tan(δ). In contrast the binder without plasticizer has the highest $T_g$ value but interestingly not much more than the ADN formulations.

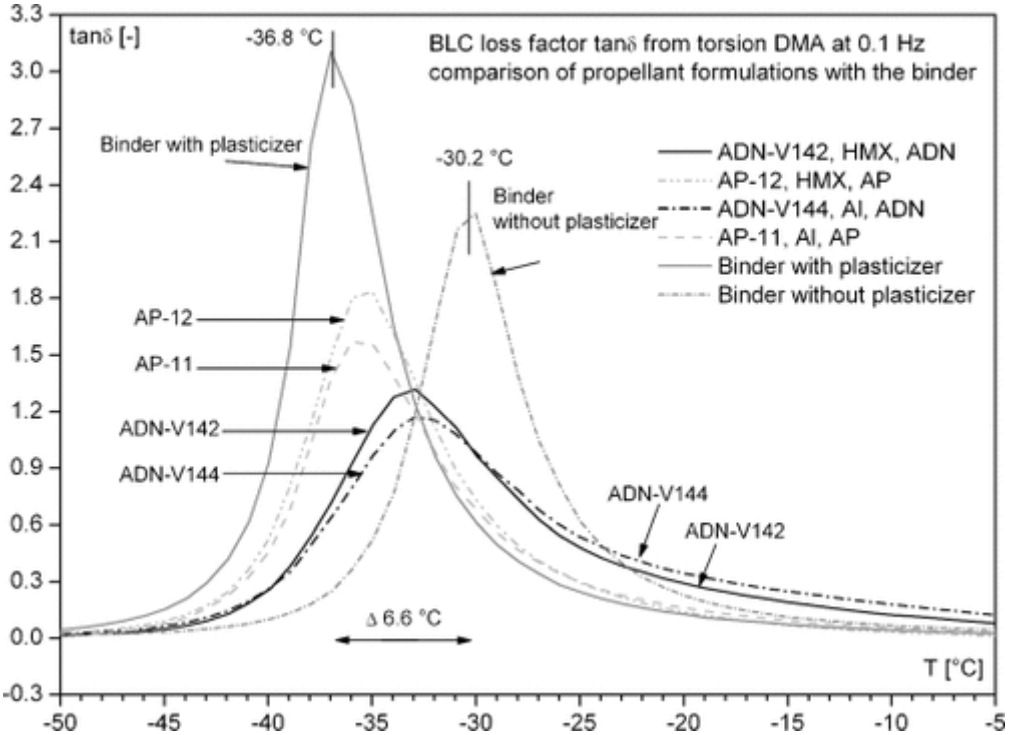

Figure 1 Baseline corrected loss factor (tan(δ)) curves of the unaged y-xx propellant formulations and their binder, with and without plasticizer, tested at 0.1 Hz.

In Table 3 the volume fractions of the main ingredients of the four formulations are compiled. The differences between the volume fractions of the solid loads are quite small. Therefore one can conclude that the differences in volume fractions cannot cause the differences in loss factor intensity and peak temperature values.

Table 3. Composition of the investigated formulations in % volume fraction.

| | **ADN-V142** | **AP-12** | **ADN-V144** |
|---|---|---|---|
| ADN | 48.95 | – | 50.06 |
| AP | – | 47.22 | – |
| HMX | 8.11 | 8.39 | – |
| Al | – | – | 6.02 |
| Total filler | 57.06 | 55.61 | 56.08 |
| Desmophen® D2200 | 23.48 | 24.28 | 24.02 |
| Desmodur® N3400 | 5.64 | 5.83 | 5.77 |
| HX-880 | 0.17 | 0.18 | 0.17 |
| TMETN | 11.77 | 12.16 | 12.04 |
| Stabilizers | 1.88 | 1.94 | 1.92 |
| Total binder | 42.94 | 44.39 | 43.92 |
| Total | 100.0 | 100.0 | 100.0 |

All the $T_g$ values can be found in a relatively narrow range of 6.6 °C. The cause is the strong intermolecular interaction between all the substances, which limits the molecular mobility of the polymer chains. AP-xx propellants show lower glass transition temperature values than the corresponding ADN formulations. The same results were also obtained with DSC measurements ($T_{g,\mathrm{DSC}}$) (Table 4, Table 5). The values of the D2200xx formulations are 40 °C higher than the ones of the AP/HTPB-based formulations which show −82 to −83 °C for $T_{g,\mathrm{DSC}}$ [19]. Due to the high glass transition temperature values, the y-xx formulations may be of limited use for military in-service with regard to the climatic conditions specified in a NATO STANAG [20], but they can be suitable for space launch boosters [2, 21].

Table 4. Glass transition temperature values ($T_{g,\mathrm{DSC}}$) of unaged and aged AP-xx propellants determined with DSC.

| **Propellant** | **Filler** | $\boldsymbol{T_{g,\mathrm{DSC}}}$ | | | |
|---|---|---|---|---|---|
| | | **Unaged** | **85 °C, 12 d** | **70 °C, 20 d** | **65 °C, 47 d** |
| AP-11 | µAl | −41.47 | −40.99 | −41.25 | −42.78 |
| AP-12 | HMX | −42.61 | −41.82 | −41.20 | −41.61 |

Table 5. Glass transition temperature values ($T_{g,\mathrm{DSC}}$) of unaged and aged ADN-xx propellants determined with DSC.

| **Propellant** | **Filler** | $\boldsymbol{T_{g,\mathrm{DSC}}}$ | | | |
|---|---|---|---|---|---|
| | | **Unaged** | **85 °C, 12 d** | **70 °C, 15 d** | **65 °C, 23.5 d** |
| ADN-V142 | HMX | −39.87 | −42.58 | −42.89 | −40.98 |
| ADN-V144 | µAl | −39.41 | −41.17 | −39.01 | −39.84 |

The loss factor is a composed distribution function (non-normalized density function) describing the distributions of the glass transitions of the structural elements of the polymer network in the formulations. If the transitions are deformation frequency (rate) dependent, they are so-named relaxation transitions, which shift to higher temperature with increasing deformation frequency [22, 23] The relaxation meant here is the molecular reorientation process in going from lower to higher temperatures, which means the condition for the minimal free enthalpy changes and the system "relaxes" to the new equilibrium condition [24]. The shift to higher temperatures with increasing deformation rate is caused by strain rate hardening of the material. This phenomenon is in contrast to melting and softening processes, crystallization, and chemical reactions, which are not deformation

rate or frequency dependent [23]. All the ADN- and AP-based materials showed evidence of this strain rate dependence. In contrast to the AP/HTPB-based materials, the intensity of the loss factor peak decreases with frequency [16]. The glass transition temperatures found with GAP-BPS systems are in the range of −28 °C to −24 °C [7], and this in spite of using BDNPA-F as plasticizer, which has a lower melting temperature than TMETN, namely −15 °C versus −3 °C.

Table 6 lists the $T_g$ values determined by DMA at the applied deformation frequencies. The deformation frequency dependence of the thermally activated molecular reorientation processes was analyzed by an Arrhenius type equation (for details please refer to a previous publication [25]). This dependency allows the estimation of the apparent activation energy ($E_a$*) of the underlying relaxation processes [26, 27]. Values of $E_a$*, reported in Table 7, are higher compared with the AP/HTPB-based formulations [25], which are in the range of 140 to 160 kJ mol$^{-1}$ for the unrestricted binder transition. The replacement of Al by HMX increases the $E_a$* values. Not only the filler but also the type of oxidizer has a recognizable effect. The replacement of ADN by AP increases the apparent activation energy of about 20 kJ mol$^{-1}$. Generally one concludes that the less distortion or hindrance is imposed by the fillers on the binder, the more pronounced is the strain rate hardening. This is in line with the increase in $E_a$* value for the pure binder. The binder formulation without plasticizer has the highest $E_a$* value. This means that the binder is completely undisturbed and the energetic interactions between the polymer chains are higher than with plasticizer. Similar behavior is found with HTPB-based CRP (Table 7). Because in HTPB binders the dispersion forces are dominant, the interaction energies and in turn the $E_a$* values are smaller. But again the binder shows higher $E_a$* values than the corresponding propellant formulation.

Table 6. Glass transition temperature values ($T_{g,DMA}$) [°C] of unaged ADN-xx and AP-xx formulations as well as of the binder with and without plasticizer, determined with torsion DMA.

| Deform. frequency | ADN-V142 | AP-12 | ADN-V144 | Binder with plast. | Binder without plast. |
|---|---|---|---|---|---|
| 0.1 Hz | −33.16 | −35.36 | −32.67 | −36.82 | −30.2 |
| 1.0 Hz | −29.60 | −32.11 | −28.90 | −33.97 | −27.76 |
| 10 Hz | −24.98 | −27.84 | −24.23 | −30.27 | −23.97 |
| 30 Hz | −22.25 | −25.46 | −21.56 | −27.91 | −21.82 |

Table 7. Apparent activation energy ($E_a$*) of the Arrhenius evaluation of the shift of the peak temperature loss factor by deformation frequency of the unaged y-xx propellant formulations and of the binder with and without plasticizer (TMETN). For direct comparison the data of HTPB-based CRP AV04 [13] and also of the HTPB binder with and without plasticizer are included.

| Propellant | Filler | $E_a$*($T_g$) [kJ mol$^{-1}$] | log [$f_0$($T_g$)] [Hz] |
|---|---|---|---|
| ADN-V142 | HMX | 261 ± 14 | 55.93 ± 3.1 |
| ADN-V144 | μAl | 258 ± 11 | 55.13 ± 2.4 |
| AP-11 | μAl | 277 ± 16 | 59.87 ± 3.3 |
| AP-12 | HMX | 281 ± 15 | 60.77 ± 3.2 |
| D2200 binder with plasticizer | – | 309 ± 20 | 67.30 ± 4.4 |
| D2200 binder without plasticizer | – | 348 ± 21 | 74.26 ± 4.5 |
| AV04 (CRP with HTPB binder) | AP, Al | 149 ± 9 | 38.55 ± 2.3 |
| HTPB-binder with plasticizer | – | 196 ± 10 | 51.02 ± 2.6 |
| HTPB-binder without plasticizer | – | 211 ± 16 | 52.88 ± 4.0 |

Figure 2 shows the aging behavior of the propellant formulations followed by the changes in loss factor. For every aging time the presence of one apparent maximum in the loss factor curve can be observed. The thermal history of the material has influences on the behavior and shape of the apparent

peak of the loss factor curve. The energy transferred to the sample during the DMA measurements is partly transmitted loss free from the donor side to the acceptor side of the specimen holder and partly used-up by the propellant specimen. This second part has two contributions: a purely dissipative one, in which the energy is transformed to heat by frictional effects inside the sample, and a contribution used for the molecular rearrangements of the binder network. To discuss the changes in loss factor only such parts will and should be considered, which reflect the molecular rearrangement processes. Moreover, to quantify these changes, it is necessary to remove the dissipative effects not belonging to the molecular rearrangements of the binder network by applying a suitable iterative baseline correction function. Then the obtained loss factor curve is modeled in order to separate the parts reflecting different binder mobility, which can be aging sensitive in distinct ways. The procedure used was discussed in a previous paper [13]. An example of the corrected loss factor curve and of the iterative baseline correction procedure is presented in Figure 3.

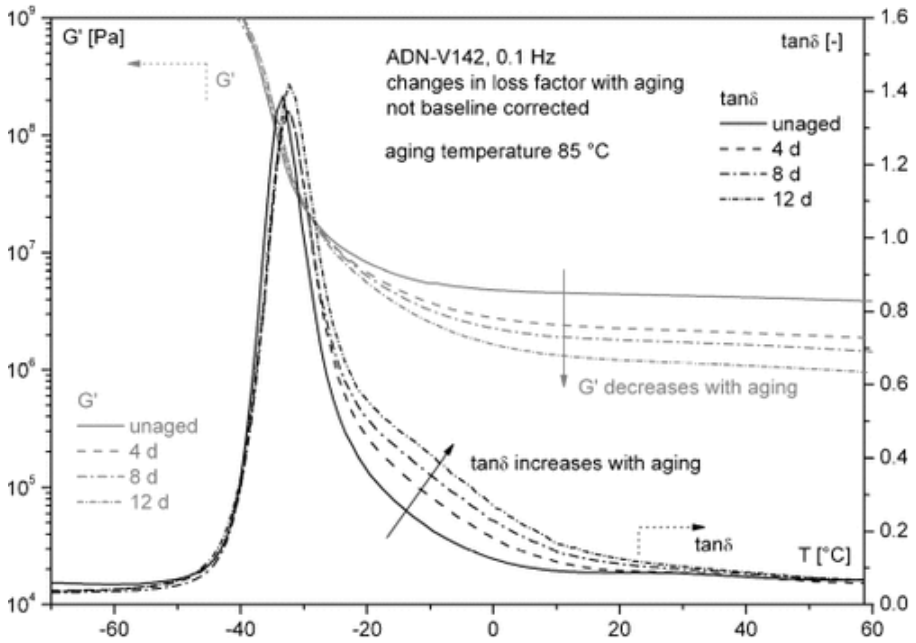


Figure 2 Loss factor tan(δ) and storage modulus G′ vs. measurement temperature for ADN-V142 propellant formulation as function of aging time at 85 °C.

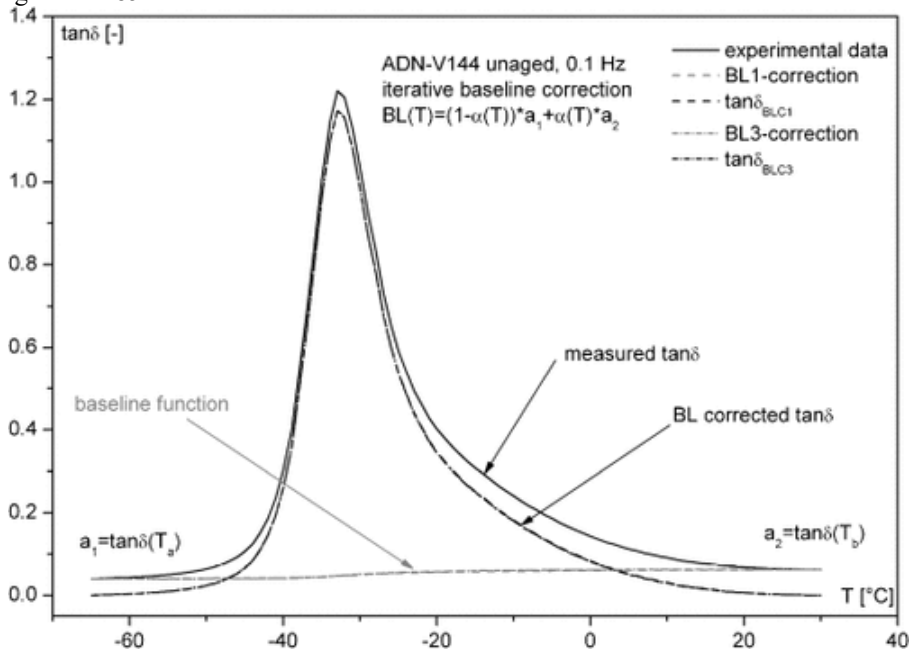


**Figure 3** Baseline correction of the loss factor of the ADN-V144 unaged propellant formulation.

The AP-based formulations show only a decrease of the height of the maximum of tan(δ) with aging and peak width changes or peak maximum shifts were not observed (Figure 4). Instead, the positions of the peak of the ADN-xx formulations were influenced. The considerations related to $T_g$ agree with the DSC measurements of the aged materials (Table 4, Table 5). Figure 2 and Figure 4 present other interesting features characterizing the ADN-based propellants: the width of the loss factor curves increases with aging and the intensity of the high temperature side increases also. Moreover, the storage modulus (G′) decreases with aging. These materials show a significantly different aging behavior compared with the AP/HTPB-based propellants [13]. The observed trend can be explained as chain scission [28] and dewetting phenomena [29] and the cause of it can be definitely attributed to the presence of ADN instead of AP.

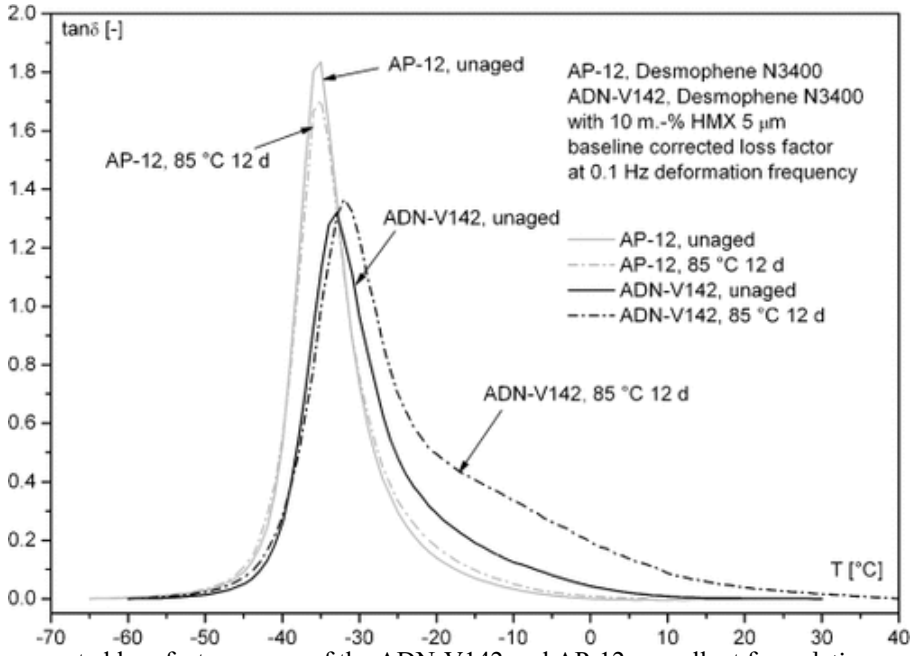

Figure 4 Baseline corrected loss factor curves of the ADN-V142 and AP-12 propellant formulations, unaged and aged at 85 °C over 12 d and tested at 0.1 Hz.

After this first step in data analysis, the baseline corrected curves were modeled by the exponentially modified Gauss distribution function (EMG) [27], which is a convolution between an exponential function and a Gaussian distribution. A previous study described and analyzed the entire procedure in details [13], while several types of distributions functions were analyzed in another paper [30]. Loss factor curves of the ADN-based propellants were modeled with two EMGs using Equation (1). A detailed description of the parameters used in the EMG modeling can be found in Ref. 13. An example of the description of the loss factor is shown in Figure 5. The dissipative parts during the rearrangement processes, characteristic for the molecular structure of the ingredients of the propellant formulation, can be analyzed by plotting the formal Gauss peaks contained in the EMG and the EMG peaks itself of all the molecular transitions. Details can be found in Ref. 31.

$$\tan\delta_{BLC} = td_0 + \sum_{i=1}^{N} \frac{A_i}{\tau_i} \cdot \frac{1}{2} \cdot \exp\left[0.5 \cdot \left(\frac{w_i}{\tau_i}\right)^2 - \frac{T - Tc_i}{\tau_i}\right] \cdot \left\{1 - erf\left[-\frac{1}{\sqrt{2}} \cdot \left(\frac{T - Tc_i}{w_i} - \frac{w_i}{\tau_i}\right)\right]\right\} \quad (1)$$

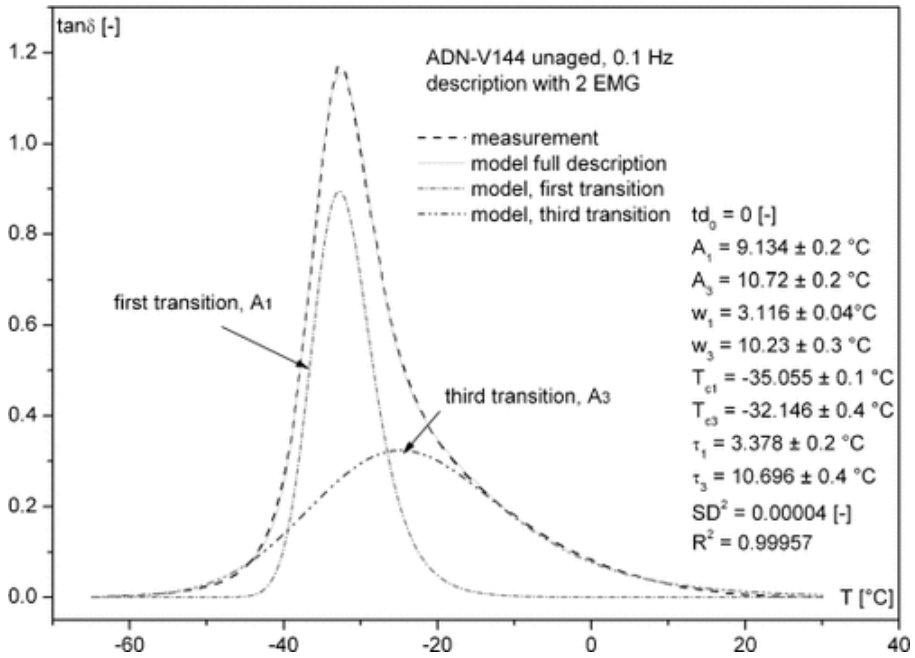

Figure 5 Description of the loss factor of the unaged ADN-V144 propellant formulation with two EMG functions.

In order to be consistent with the nomenclature used with the AP/HTPB/Al propellant formulations (AVxx) for the loss factor structure and due to the absence of a second apparent peak, the two transitions of the ADN-D2200xx propellants were named first and third, because the high temperature transition of these materials behaves similarly to the third transition of the AP/HTPB/Al ones. Peak 1 represents the main transition peak of the elastomeric polyesterurethane. It does not show changes with aging, whereas peak 3 is related to the restricted polymer shell around the ADN particles and it shows changes caused by chain scission and/or dewetting phenomena. Previous mass loss investigations [7] compared the aging behavior of ADN prills with the aging of the ADN- and AP-Desmophen®-based formulations. The role of ADN in the decomposition process of the material was evident. Measurements of mass loss revealed an acceleratory behavior, which is in part caused also by autocatalysis. Mass loss values were below of the pure ADN ones due to a less ADN content in the formulations. In conclusion, ADN decomposes and shrinks in diameter during aging (Figure 9), therefore also dewetting occurs. This phenomenon questions also the usefulness of coating of ADN prills.

Two parameters of the EMG modeling were considered: $A_i$ (peak areas of the EMG peaks *i*, also equal to the area of the Gauss peaks *i* alone [°C]) and $Tc_i$ (temperature [°C] at peak maxima of the Gaussian part *i*). By plotting the values of the peak areas vs. the aging times, different tendencies can be observed (Figure 6). The area $A_1$ of the first transition stays quite constant with aging, area $A_3$ increases instead. The change rate of $A_3$ can be described by a formal rate equation of zero order for the considered aging range (Equation (2)) [13].

$$\left(\frac{d(A_3(t,T))}{dt}\right)\Bigg|_T = S \cdot k_{A_3}(T) \qquad (2)$$

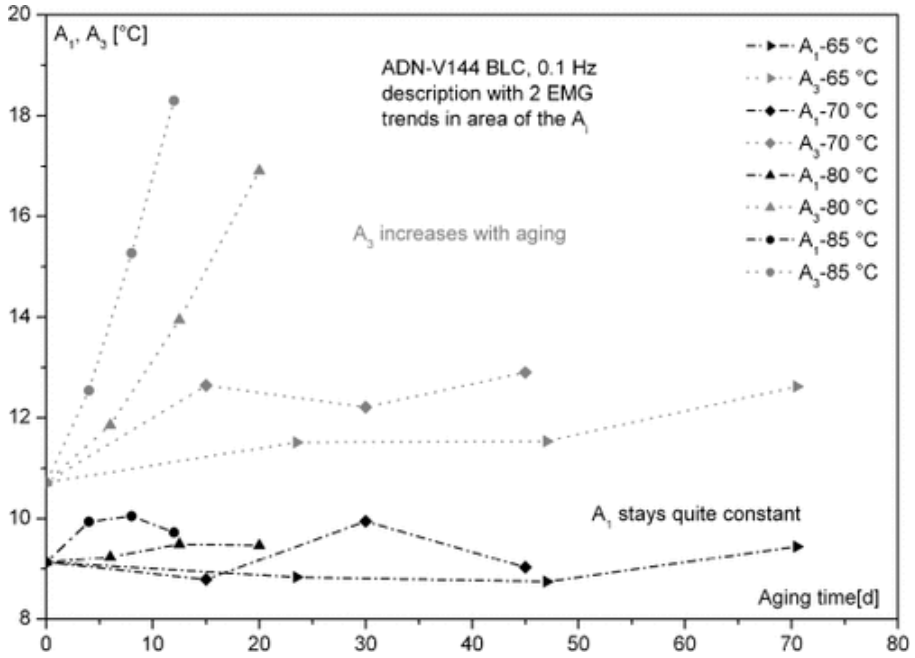

Figure 6 Trend of the peak areas ($A_1$, $A_3$) with aging time for the ADN-V144 propellant formulation.

where $k_{A_3}(T)$ is the change rate constant for area $A_3$ [°C $d^{-1}$]. S is the sign factor: S is −1 for decreasing area with time, S is +1 for increasing area with time.
The integration of Equation (2) gives:

$$A_3(t,T) = A_3(0) + S\ k_{A_3}(T)\ t, \quad \text{with} \quad (S = +1) \tag{3}$$

A linear dependence of $A_3(t)$ with aging time was observed (Equation (3)). By plotting the natural logarithm of the change rate constant, $\ln(k_{A_3})$ vs. $1/T$ (temperature in Kelvin) (Equation (4)), values of the activation energies $E_a(A_3)$ are obtained (Table 8).

$$\ln(k_{A_3}) = \ln(Z(A_3)) - \frac{E_a(A_3)}{R}\ \frac{1}{T} \tag{4}$$

Table 8. Arrhenius parameters for the rate constants of change in peak areas $A_3$ with aging for the ADN-xx formulations.

| **Propellant** | ***A*3(0) [°C]** | **$E_a(A_3)$ [kJ mol$^{-1}$]** | **log ($Z(A_3)$ [°C d$^{-1}$])** | **$R^2[A_3]$)** |
|---|---|---|---|---|
| ADN-V142 | 10.22 | 171.4 ± 21 | 24.706 ± 3.1 | 0.9721 |
| ADN-V144 | 10.72 | 162.2 ± 2.0 | 23.446 ± 0.31 | 0.9997 |

They are significantly higher than the activation energies obtained for the AP/HTPB/Al propellants, which are in the range 70–85 kJ mol$^{-1}$ [13]. A possible interpretation can be referred to the fact that some parts of ADN establish permanent dipole to permanent dipole interactions with the binder (carboxyl groups of the polyesterurethane interact with $NO_2$ groups of ADN) and also to ionic-type interactions at the surface of the ADN prills, especially coming up with the decomposition processes of the ADN. The decomposition reactions of ADN can have $E_a$ values within the range found herein [32, 33]. One may conclude that the controlling process is ADN decomposition.
Also the temperature values $T_{c_i}$ show an aging trend (Figure 7). Whereas the temperature of the first transition ($T_{c_1}$) stays quite constant with aging, $T_{c_3}$ increases with the aging time. This may be caused by the broadening of the peak $A_3$, which can shift the maximum slightly to higher temperatures.

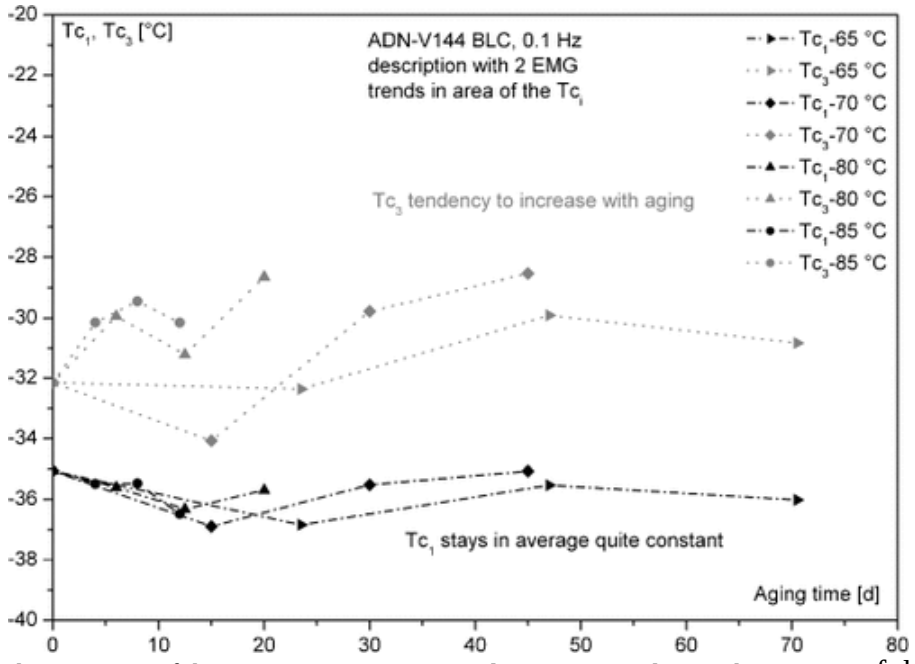

Figure 7 Trend with aging time of the transition temperature values corresponding to the maxima of the peak transitions in the Gaussian parts of EMG of the ADN-V144 propellant formulation.

The procedure used for the analysis of the DMA data pointed out the possibility of extracting information on the aging process from the loss factor curve. The considered EMG modeling is not specific to a particular formulation, but it was used for different materials as reported in Refs. [13, 17, 24, 27]. As with the HTPB-based CRP the main peak of the loss factor does not change in maximum temperature. This means this part of the glass-rubber transition range represented in loss factor cannot be used as an aging indicator. Moreover, with DSC one recognizes only the main glass-rubber transition of the binder, not the secondary ones, as here with the hidden peak $A_3$. The same holds with HTPB propellants. The consequence is that the aging of CRP cannot be followed by the glass-rubber transition temperatures determined with DSC.

## 3.2 SEM Investigations

Binder and/or oxidizer modifications with time and temperature were analyzed with SEM measurements. At low magnification (100×) no morphology variations were observed. At higher magnification (300×), ADN particles showed morphological changes (Figure 9) with respect to the unaged condition (Figure 8). SEM micrographs of the unaged ADN prills show particles having a spherical shape and a smooth particle surface [34, 35]. Micrographs have also revealed the presence of some voids inside the unaged prills (Figure 8). Analyses published in previous publications have also given evidence of these voids [16, 35].

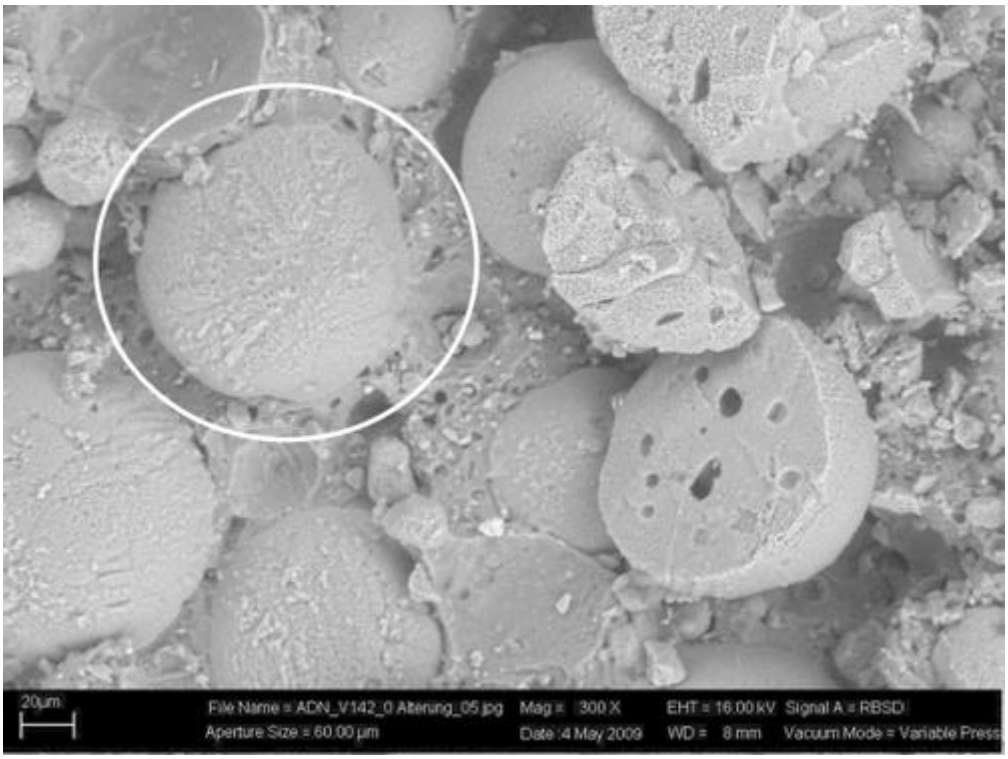

Figure 8 SEM micrograph of the surface of the unaged ADN-V142 propellant (300×).

Further efforts are made to reduce the filler porosity by using effective stabilizers for ADN and applying suitable process technology, e.g. fluidized bed technology [36]. Some streaks can be already recognized at the surface of the prills of the unaged formulation (Figure 8). With aging time, the number and dimensions of the streaks increase, leading to particles having a type of grooved surface. At high aging temperature (80 °C) the oxidizer particles show grooves in an arrangement similar to a football (Figure 9).

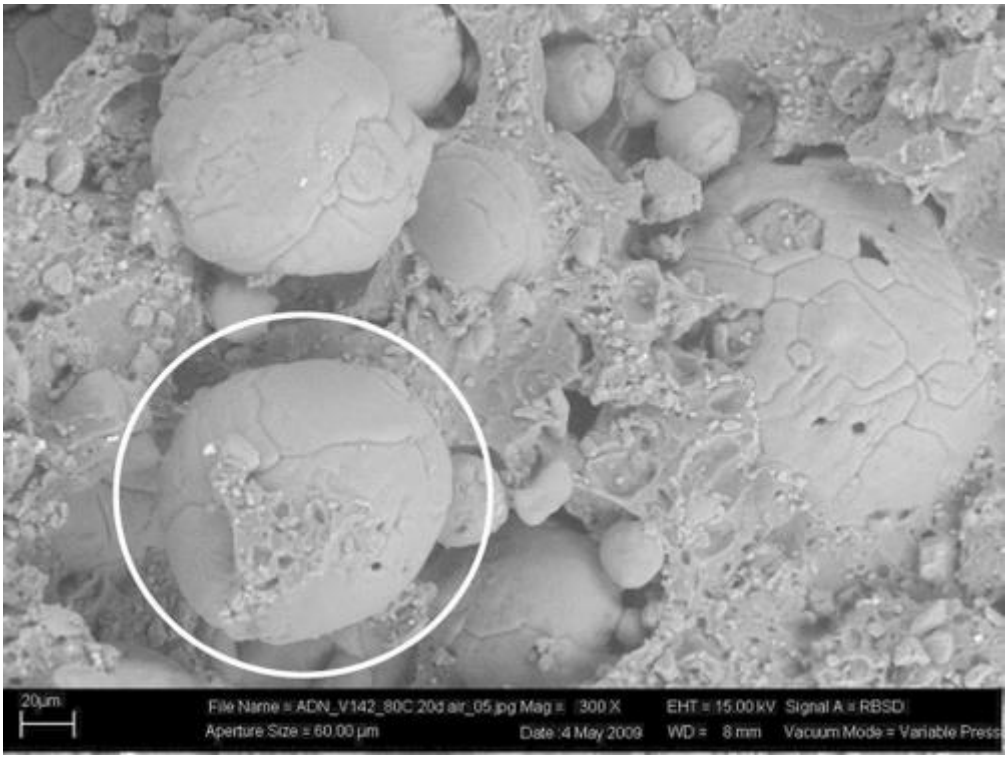

Figure 9 SEM micrograph of the surface of the aged ADN-V142 propellant (300×); aging was at 80 °C, 20 d.

# 4 Conclusions

The study has focused on the aging investigation of the surface-layer of ADN and AP propellants with a Desmophen®-based (type D2200) polyurethane binder, but only the ADN-xx formulations were subjected to an extensive aging program. No possible plasticizer migration and debonding (grain-liner) effects were included. The accelerated aging temperature range was between 65 °C and 85 °C, in air, with aging time intervals adjusted to a thermal equivalent load of 15 years at 25 °C. For this correlation the generalized van't Hoff rule was applied with a scaling factor F=2.9 per 10 °C temperature change. Whereas the AP-based formulations show only very small changes by aging, the ADN-xx propellants show very significant variations in mass loss and in DMA loss factor. The glass transition temperature values of the main transition determined by DMA and DSC measurements indicate that the ADN-formulations cannot be used for the very broad in-service temperature range for defense systems (−54 °C to +71 °C) 20. Some effect of the oxidizer on the glass transition temperature was recognized: by replacing ADN by AP the glass transition temperature values decrease by 2 to 3 °C and the tan (δ) peak width decreased. This can be caused by the stronger energetic interaction between ADN and binder chains resulting in more mobility restrictions.

Loss factor curves exhibit only one main apparent peak but the modeling with EMG functions revealed also the presence of a second "hidden" one. Therefore, two main relaxation processes characterize the formulations. The first peak represents the main transition peak of the elastomeric polyester urethane binder and the hidden one is related to binder shell around the filler particles.

One important result is that with aging the main peak does not change in area and maximum temperature but the second peak does. This means the glass transition temperatures determined by DSC will not indicate an aging effect, because DSC "sees" only the main transition. This is because DSC recognizes transitions only when greater changes in the specific heats occur. This is not the case in the secondary transitions in HTPB and Desmophen® binders and in their polymer shells formed around the filler particles.

The other important result is the change in area and maximum temperature of the hidden peak. Especially the area $A_3$ increases significantly with ADN-D2200 formulations. Nothing similar happened with the AP-D2200 formulations. Because the storage modulus decreased it is concluded that this change in $A_3$ is caused by the chain scission of the binder, but also by dewetting phenomena in the polymer shell, because of shrinking of the ADN prills together with the attack of decomposing ADN on the binder. Due to the time-temperature dependence of the area $A_3$ in the loss factor curve, obtained by EMG modeling, an Arrhenius parameterization was possible and the activation energies of the ADN-based formulations were obtained. In comparison with the AP/HTPB/Al-based propellants (AVxx [13]) the changes in area $A_3$ of the ADN-D2200xx propellants are characterized by a much higher activation energy range: $E_a(A_3)_{AVxx}$= 70 to 95 kJ mol$^{-1}$ for the AVxx vs. $E_a(A_3)_{ADN-D2200xx}$=162 to 171 kJ mol$^{-1}$. These last $E_a$ values coincide with the $E_a$ values of the decomposition of liquid ADN [32, 33].

Finally, some words to the meaning of the changes in the secondary transition in HTPB-AP and polyester-ADN systems. In HTPB-AP systems the secondary transitions indicate a hardening in the binder shell, which results in increase of strength but also in the decrease of strain capability. Under strain load the binder shell may be strain overloaded and the cracking of the binder is started in these regions of the propellant. This effect is increased by aging. In polyester-ADN systems the binder shell suffers from chain scissoring and weakening of the binder. Under strain load cracks are formed by stress overload because of reduced strength of the binder. Therefore these secondary transitions are valuable aging indicators. In quantitative correlation with the corresponding areas of the loss factor curves the aging state is predictable.

## Symbols and Abbreviations

$\rho_{th}$ Mixture density based on densities of the individual ingredient determined with the ICT Thermodynamic Code [$cm^{-3}$]
ADN Ammonium dinitramide, oxidizer
$A_i$ Peak areas of the EMG peaks *i* [°C]
Al Aluminum, fuel
μAl Aluminum with particles size in μm range
AP Ammonium perchlorate, oxidizer
AVxx CRP type based on HTPB, Al, AP 13
BDNPA-F 1 : 1 mixture of bis(2,2-DiNitroPropyl)Acetal and bis(2,2-dinitropropyl)Formal, energetic plasticizer or energetic liquid filler
BPS BisPropargylSuccinate, curing agent; curing based on the Huisgen reaction between ethine group and organic azide;
CRP Composite rocket propellant
DMA Dynamic mechanical analysis
DSC Differential scanning calorimetry
D2200 Polyesterpolyol, PUR prepolymer, based on ester condensation of adipic acid and diethylene glycol
$E_a$ Activation energy [kJ $mol^{-1}$]
$E_a$* Apparent activation energy [kJ $mol^{-1}$]
EMG Exponentially Modified Gauss distribution
G′ Storage shear modulus [Pa]
G″ Loss shear modulus [Pa]
GAP Glycidyl Azide Polymer, PUR pre-polymer
GvH Generalized van't Hoff rule
HMX Octogen, energetic filler
HTPB Hydroxyl terminated polybutadiene, pre-polymer
HX-880 Bonding agent, *N*,*N*-bis(2-hydroxyethyl) glycolamide, referred as BHEGA
ICM Intercontinental missile (ballistic rocket) also ICBM
m.-% Mass-%, mass content by percent
NATO North Atlantic Treaty Organization
NCO Isocyanate group
$NO_2$ Nitrogen dioxide
O.B. Oxygen balance
OH Hydroxyl functional group
PID Proportional-integral-differential
PUR Abbreviation for polyurethane
$R_{eq}$ Equivalent ratio between the functional groups of curing agent and binder
RH Relative humidity
SEM Scanning electron microscopy
SLBM Ship (submarine) launched ballistic missile
tan(δ Loss factor
$Tc_i$ temperature at peak maxima in the Gaussian part i of EMG [°C]
$T_g$ Glass transition temperature [°C]
$T_{g,DMA}$ Glass transition temperature, determined as maximum temperature of the loss factor curve (means the main transition of the binder) [°C]
$T_{g,DSC}$ Glass transition temperature determined from DSC measurements [°C]
TEL Thermal equivalent load
TMETN Trimethylolethyltrinitrate, plasticizer or energetic liquid filler.

## Acknowledgements

This work was carried out as part of the PhD Thesis of Sara Cerri performed at Politecnico di Milano, Energy Dept., Italy and Fraunhofer ICT, Germany 18. Authors would like to thank both institutions.

## References

1. United States Environmental Protection Agency, Perchlorate Treatment Technology Update, Washington D.C., USA, May, 2005
2. High Performance Solid Propellants for In-Space Propulsion (HISP), FP7 project, reference No. 262099
3. M. Johansson, J. De Flon, A. Petterson, M. Wanhatalo, N. Wingborg, Spray Prilling of ADN and Testing of ADN-Based Solid Propellants, 3rd Int. Conference on Green Propellants for Space Propulsion, Poitiers, September 17-20, France, 2006.
4. M. Y. Nagamachi, J. I. S. Oliveira, A. M. Kawamoto, R. L. Dutra, ADN - The New Oxidizer around the Corner for an Environmentally Friendly Smokeless Propellant, J. Aerosp. Technol. Management- 2009, 1, 153-160.
5. A. Larsson, N. Wingborg, Green Propellants Based on Ammonium Dinitramide (ADN), in: Advances in Spacecraft Technologies (Ed.: J. Hall). Web-based Access: InTech, 2011, DOI: 10.5772/13640.
6. D. E. G. Jones, Q. S. M. Kwok, M. Vachon, C. Badeen, W. Ridley, Characterization of ADN and ADN-Based Propellants, Propellants Explos. Pyrotech. 2005, 30, 140- 147.
7. S. Cerri, M. A. Bohn, K. Menke, L. Galfetti, Characterization of ADN/GAP-based and ADN/Desmophen®-Based Propellant Formulations and Comparison with AP Analogues, Propellants Explos. Pyrotech.- 2014, 39, 192-204.
8. E. Landsem, T. L. Jensen, F. K. Hansen, E. Unneberg, T. E. Kristensen, Mechanical Properties of Smokeless Composite Rocket Propellants Based on Prilled Ammonium Dinitramide, Propellants Explos. Pyrotech. 2012, 37, 691- 698.
9. K. Menke, T. Heintz, W. Schweikert, T. Keicher, H. Krause, Formulation and Properties of ADN/GAP Propellants, Propellants Explos. Pyrotech. 2009, 34, 218- 230.
10. M. A. Bohn, Prediction of Equivalent Time-temperature Loads for Accelerated Ageing Conditions to Simulate Preset in-storage Ageing and Time-temperature Profile Loads, 40th Int. Annual Conference of ICT, Karlsruhe, Germany, June 23-26, 2009, paper 78.
11. U. Ticmanis, S. Wilker, G. Pantel, M. Kaiser, P. Guillaume, C. Balès, N. van der Meer, Principles of STANAG for the Estimation of the Chemical Stability of Propellants by Heat Flow Calorimetry, 31st Int. Annual Conference of ICT, Karlsruhe, Germany, June 27-30, 2000.
12. M. Celina, K. T. Gillen, R. A. Assink, Accelerated Aging and Lifetime Prediction: Review of non-Arrhenius Behaviour due to Two Competing Processes, Polym. Degrad. Stab.- 2005, 90, 395-404.
13. S. Cerri, M. A. Bohn, K. Menke, L. Galfetti, Aging of HTPB/Al/AP Rocket Propellant Formulations Investigated by DMA Measurements, Propellants Explos. Pyrotech. 2013, 38, 190- 198.
14. STANAG 4581, Explosives, Assessment of Ageing Characteristics of Composite Propellants Containing an Inert Binder, Military Agency for Standardization, NATO, Final Draft Edition, 2003.

15. T. Heintz, W. Reinhard, C. Birke, K. Leisinger, Adjustment of the Particle Size of ADN-Prills Generated by the Emulsion Crystallization Process, 44th Int. Annual Conference of ICT, Karlsruhe, Germany, June 25-28, 2013, paper 73.
16. S. Cerri, M. A. Bohn, Ageing Behavior of Rocket Propellant Formulations with ADN as Oxidizer, Proc. 14th Int. Seminar New Trends and Research in Energetic Materials, Pardubice, Czech Republic, April 13-15, 2011, 89-105.
17. G. Mußbach, M. A. Bohn, Impact of Ageing on the Loss Factor of Composite Rocket Propellants and Interpretation of Changes Considering Post-curing, 16th Int. Seminar New Trends and Research in Energetic Materials, Pardubice, Czech Republic, April 10-12, 2013, 280-293.
18. S. Cerri, Characterisation of the Ageing of Advanced Solid Rocket Propellants and First Step Design of Green Propellants, PhD Thesis, Politecnico di Milano, Dipartimento di Energia, Dottorato di Ricerca in Energetica, XXII Ciclo, 2011.
19. S. Cerri, M. A. Bohn, K. Menke, L. Galfetti, Ageing Behaviour of HTPB Based Rocket Propellant Formulations, Cent. Eur. J. Energ. Mater. 2009, 6, 149- 165.
20. Military Agency for Standardization, Extreme Climatic Conditions and Derived Conditions for Use in Defining Design/test Criteria for NATO Forces Material, STANAG 2895, Edition 1, February 15, 1990.
21. F. Lillo, B. D'Andrea, G.Marcelli, A. Sebasta, Long Term Aging of Aerospace and Tactical SRM. Experimental Study, 37th AIAA/ASME/SAE/ASEE Joint Propulsion Conference and Exhibit, Salt Lake City, USA, July 8-11, 2001, paper AIAA 2001-3284.
22. G. W. Ehrenstein, G. Riedel, P. Trawiel, Praxis der Thermischen Analyse von Kunststoffen, Carl Hanser Verlag, Munich, 2003.
23. G. Widmann, J. Schawe, R. Riesen, Interpreting DMA Curves, Part 1, Thermal Analysis UserCom 15, Mettler Toledo, January, 1-6, 2002.
24. M. A. Bohn, G. Mußbach, S. Cerri, Influences on the Loss Factor of Elastomer Binder and its Modeling, 43rd Int. Annual Conference of ICT, Karlsruhe, Germany, June 26-29, 2012, paper 60.
25. S. Cerri, M. A. Bohn, K. Menke, L. Galfetti, Ageing Behaviour of HTPB Based Rocket Propellant Formulation, Cent. Eur. J. Energ. Mater. 2009, 6, 149- 165.
26. J. L. De la Fuente, M. Fernández-García, M. L. Cerrada, Viscoelastic Behavior in a Hydroxyl-Terminated Polybutadiene Gum and its Highly Filled Composites: Effect of the Filler Type on the Relaxation Processes, J. Appl. Polym. Sci.- 2003, 88, 1705-1712.
27. G. Tsagaropoulos, A. Eisenberg, Dynamical Mechanical Study of the Factors Affecting the Two Glass Transition Behavior of Filled Polymers. Similarities and Differences with Random Ionomers, Macromolecules 1995, 28, 6067- 6077.
28. A. Kumar, S. Commereuc, V. Verney, Ageing of Elastomers: A Molecular Approach based on Rheological Characterization, Polym. Degrad. Stab.- 2006, 85, 751-757.
29. A. Lepie, A. Adicoff, Dynamic Mechanical Behavior of Highly Filled Polymers: Dewetting Effect, J. Appl. Polym. Sci.- 1972, 16, 1155-1166.
30. S. Cerri, M. A. Bohn, K. Menke, L. Galfetti, Ageing Behavior of Composite Rocket Propellant Formulations, 3rd European Conference for Aerospace Science (EUCASS), Versailles, France, July 6-9, 2009, paper 98.
31. S. Cerri, M. A. Bohn, Ageing Behaviour of Rocket Propellant Formulations with ADN as Oxidizer Investigated by DMA, DSC, and SEM, 42nd Int. Annual Conference of ICT, Karlsruhe, Germany, June 28-July 1, 2011, paper 42.

32. M. A. Bohn, J. Aniol, H. Pontius, J. Hürttlen, Thermal Stability and Stabilization of ADN-Water Gels, 38th Int. Annual Conference of ICT, Karlsruhe, Germany, June 26-29, 2007, paper 4.
33. M. A. Bohn, P. Gerber, Stabilization of Solid and Liquid ADN-Aluminum Mixtures. Suitable Stabilizing Substances Investigated by Heat Generation Rate, Mass Loss and Product Analyses, EuroPyro 2007 combined with 34th Int. Pyrotechnics Seminar, Beaune, France, October 8-11, 2007, pp. 148-160.
34. T. Heintz, K. Leisinger, H. Pontius, Coating of Spherical ADN Particles, 37th Int. Annual Conference of ICT, Karlsruhe, Germany, June 27-30, 2006, paper 150.
35. T. Heintz, H. Pontius, J. Aniol, C. Birke, K. Leisinger, W. Reinhard, Ammonium Dinitramide (ADN)-Prilling, Coating and Characterization, Propellants Explos. Pyrotech. 2009, 34, 231-238.
36. T. Heintz, K. Leisinger, M. A. Bohn, Advanced Stabilization of ADN-Prills by Preparation of Raw Materials by Means of Fluidized Bed Technology, 43rd Int. Annual Conference of ICT, Karlsruhe, Germany, June 26-29, 2012, paper 36.